Biol. Cybern. 73, 389–400 (1995)

Biological Cybernetics

Local lateral inhibition: a key to spike synchronization?

Alfred Nischwitz [1], **Helmut Glünder** [2]

[1] Lehrstuhl für Nachrichtentechnik, Technische Universität München, Arcisstraße 21, D-80333 München, Germany
[2] Institut für Medizinische Psychologie, Ludwig-Maximilians-Universität, Gœthestraße 31, D-80336 München, Germany

Received: 12 January 1994/Accepted in revised form: 25 April 1995

Abstract. Starting from the idea that neural group activity as such is unlikely to be immediately relevant for neural synchronization, we investigate mechanisms that act at the level of individual nerve impulses (spikes). Hence, we consider populations of formal spike-emitting 'leaky integrate and fire' neurons instead of networks built from non-spiking oscillators. After outlining the principle of synchronization for basic forms of recurrent impulse coupling by using a pair of simplified formal neurons, we show that local lateral inhibition results in robust impulse synchronization in networks with non-vanishing transmission delays.

1 Introduction

The relevance of oscillatory and synchronous brain activity for neural information processing has been discussed over the past several decades, from the early comments of Adrian (1935), Hebb (1949) and Wiener (1961), to Pöppel (1971), Milner (1974) and Freeman (1975). These considerations originated from the observation of oscillations – such as the prominent α-rhythm – in the electroencephalogram (EEG) or similar forms of electrically recorded neural mass activity. More recently (Eckhorn et al. 1988; Gray et al. 1989), experimental evidence for stimulus-dependent synchronization of oscillatory responses in the visual cortex of the cat – mainly in the γ-band – led to a general resumption of this discussion. Currently, it is conjectured that the functional meaning of these spatio-temporal phenomena for the processing of sensory signals is to link, group or bind parts of objects according to common features.

Most of the recent investigations have used invasive measurements of local mass potentials or group activity, such as 'local field potentials' (LFP) and 'multi-unit activity' (MUA) (Engel et al. 1990). The evaluation of such single or simultaneous recordings is commonly performed by correlation, or Fourier-spectral methods which, under appropriate stimulus conditions, reveal to some extent synchrony between partly periodic activities. It has been tempting to describe and simulate the synchronization of regular LFPs by considering ensembles of coupled oscillators (Atiya and Baldi 1989; König and Schillen 1991) and that of quasi-periodic MUAs by bursting devices (Traub et al. 1987; Eckhorn et al. 1990; Bush and Douglas 1991). However, as far as it is known, LFPs and MUAs are not functional neurobiological entities in the literal sense, i.e. they do not represent signals that are processed in brain structures. Consequently, it is hard to see how neural synchronization can be realistically modelled by continuous oscillators that permanently interact. Therefore, we decided to concentrate on the underlying events of the measured composite signals, namely the spiking activity of single cells.

Although synchronization is widely associated with periodic, i.e. oscillatory, brain activity and vice versa, we suggest a distinction between periodic neural group activity that implies synchronized *and* periodic activity at the cellular level (Hebb 1949), and synchronized cellular activity that need not give rise to periodic group activity. Synchronous but aperiodic cellular activity has been reported by Engel et al. (1991). More recently these authors (Engel et al. 1993) have also emphasized the highly variable periods of recorded 'neural oscillations' and state that they must not be associated with stationary oscillations of narrow-band Fourier-spectral fundamentals. Furthermore, we found that the process of synchronization – not the state of synchrony – is supported by approximately constant stimulation and thus quasiperiodic firing of cells.

As a consequence of these ideas we wanted to know about necessary conditions for spike synchronization in locally coupled populations of formal 'leaky integrate and fire' neurons, i.e. at the 'microscopic level' (Nischwitz et al. 1991; van Hemmen et al. 1992). Today, such impulse-generating units with individual noise behaviour and stimulus-dependent impulse rate are computationally manageable even in large populations and in simulations with high temporal resolution. Different from earlier work on networks with *local excitatory* interconnections (Nischwitz et al. 1991) we focus here on

Correspondence to: H. Glünder

properties of the *local inhibitory and delayed* coupling which, from the biological point of view, represents a prominent interconnection scheme in the neocortex (Braitenberg and Schüz 1991) and has the advantage of being orders of magnitude more effective than its excitatory counterpart (Sejnowski and Lytton 1992). We imagine a population (e.g. a layer) of excitatory input units (e.g. pyramidal cells) that are reciprocally coupled via inhibitory interneurons (e.g. stellate cells). For the sake of simplicity, we neglect the interneurons and consider inhibitorily coupled input units, i.e. we assume a single spike from a single input unit to cause an inhibitory interneuron to fire – which according to Sayer et al. (1990) is indeed possible (cf. Coultrip et al. 1992).[1] In contrast to the often discussed networks with all-to-all coupling (fully interconnected) we consider a space-invariant scheme of local lateral inhibition, i.e. every unit is coupled equally to a fixed number of units in its well-defined (not random) neighbourhood; this does not imply anatomically short interconnections. Consequently, the coupling is to be termed 'functionally local'.

While there is some literature about *excitatory* spike synchronization in fully interconnected model networks (Peskin 1975; Mirollo and Strogatz 1990; Kuramoto 1991; Deppisch et al. 1992; Gerstner and van Hemmen 1992) and in locally interconnected ones (MacGregor and Palasek 1974; Hartmann and Drüe 1990; Nischwitz et al. 1991) and in networks consisting of an excitatorily coupled layer that is controlled by inhibitory interneurons (Bush and Douglas 1991; Gerstner et al. 1993a, b), we know of only a very few published studies that deal with spike synchronization by *inhibitory* coupling, namely the neuron pairs studied by Kirillov and Woodward (1993), van Vreeswijk et al. (1994) and Lytton and Sejnowski (1991; Sejnowski and Lytton 1992). All of them differ significantly from the architecture introduced here. We emphasize that, although mathematically founded and formulated, the nature of our investigations is essentially empirical. This is because exact analytical descriptions of *extended* networks with *delayed* and *local* interconnections, even between noise-free units, at best consist of combinatorially growing trees of special cases that are of limited practical value.

Although our main concern is impulse synchronization in extended populations of noisy formal neurons, we start in Sect. 2 with an explanation of general synchronization principles by the use of a minimalistic network consisting of two idealized units. In Sect. 3 we introduce the formal neuron, the network structure and objective measures of synchrony. Section 4 presents the simulation results that reveal the influence of parameter variations on the synchronization behaviour. Finally, our approach is discussed with respect to other models and to neurobiology in Sect. 5.

[1] Evidently, this assumption also dismisses the spatial integration of such interneurons. However, we found that a certain pooling of the lateral interactions does not significantly alter the properties of the proposed synchronization scheme.

2 Principles of spike synchronization

In order to communicate the basic idea of impulse synchronization between coupled integrating threshold units we consider in this section a system of only *two* coupled units of the same idealized kind that are assumed *noise-free* and that emit δ-impulses. This minimalistic configuration is commonly used for analytical investigations, such as in the pioneering work of Mirollo and Strogatz (1990) and in that of their predecessor Peskin (1975, pp 268-278). These authors show that an essential prerequisite for impulse synchronization is the 'concave down' shape of the units' temporal integration characteristic, a condition that becomes obvious from the following examples. A simple and quite natural, (and hence frequently considered) characteristic of this kind is that of a leaky integrator with constant input that we selected for our simulations (see Sect. 3.1). In their analysis of the 'two unit' system *without* delay van Vreeswijk et al. (1994) elegantly showed that synchronization can be significantly different for slowly rising postsynaptic responses.

2.1 'Two unit' system

In the first row of Fig. 1 we show the integration characteristic of the threshold unit that can be regarded as the time course of the potential $u(t)$ at the leaky cell soma or, more precisely, at the axon hillock of a formal neuron with constant current inflow. In our examples the threshold voltage θ for impulse triggering ($*$) is reached after 9 ms of continuous and *undisturbed* integration. With the emission of an impulse the potential is reset and, after a refractory interval of 1 ms, integration begins again. The dotted horizontal arrows indicate time shifts of the triggering point as they result from large and idealized steps (vertical arrows) of the soma potential that in turn are caused by received δ-impulses. Obviously, the size of the shifts depends on the temporal relation between these steps and the integration state or, in other words, on the phase with respect to the uncoupled and thus periodically firing unit. The time shift as a continuous function of the step's phase represents the so-called phase response curve, which is a functionally more adequate description of a unit's nonlinear characteristic. For a long time it has served as a standard tool in chronobiology (Pittendrigh and Bruce 1957) and has now been adopted for the analysis of neural synchronization (Cairns et al. 1993; Smith et al. 1994).

2.2 Excitatory coupling without transmission delay

In Fig. 1 we exemplify the behaviour of the four basic configurations of the idealized 'two unit' system with either excitatory or inhibitory as well as delayed or non-delayed reciprocal interconnections (Nischwitz and Glünder 1992, 1993). We start with the well-understood case of excitatory coupling without delay (Fig. 1b) where we consider unit 2 starting integrating 6.5 ms later than unit 1. Consequently, unit 1 reaches the threshold first and its immediately transmitted impulse causes unit 2

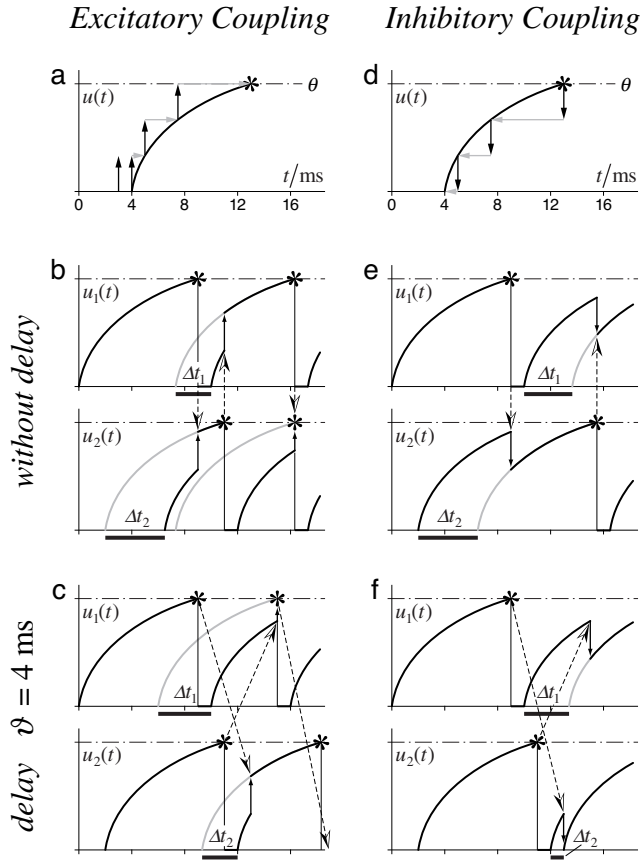

Fig. 1a–f. Four types of δ-impulse coupling between two idealized 'leaky integrate and fire' units and their synchronization behaviour. **a**, **d** The units' integration characteristic and threshold θ with time shifts of their spike triggering for various step-like changes of the potential. **b**, **c** Examples of first interactions between excitatory coupled units without and with transmission delay that produce synchronous and counterphase firing respectively. **e**, **f** Examples of first interactions between inhibitory coupled units without and with transmission delay that produce counterphase and synchronous firing respectively. For further details see text

to fire earlier (negative time shift Δt_2) than without this input impulse. The impulse from unit 2 leads to a less advanced $|\Delta t_1| < |\Delta t_2|$ triggering of unit 1 because its somatic potential $u_1(t)$ is lower than $u_2(t)$ was when unit 2 received the impulse from unit 1. Since unit 2 – which is late initially – becomes more accelerated than unit 1 the asynchrony rapidly vanishes after the exchange of a few spikes. The elegant mathematical analysis of such a configuration by Mirollo and Strogatz (1990) shows that the synchronous state is attractive except for the initial condition where the units fire exactly in counterphase, i.e. $\Delta t_2 = \Delta t_1$. Because the latter state is repellent it is irrelevant for the description of natural, i.e. noisy, systems. Although the original analysis was performed for units without a refractory period it can be shown to apply identically to units with a refractory interval.

2.3 Excitatory coupling with transmission delay

For an explanation of the excitatory coupling with delayed ($\vartheta = 4$ ms) transmission (Fig. 1c) we assume unit 2 lagging 2 ms behind unit 1. The delayed arrival of the first impulse from unit 1 at unit 2 – which itself fires even before this time – causes a smaller negative time shift Δt_2 than its response to unit 1 $|\Delta t_2| < |\Delta t_1|$ and therefore the spike events temporally diverge. Now, the synchronous state is repellent and the impulse emission in counterphase is attractive. In our example (Fig. 1c) this state is reached after only two interactions. Depending on the coupling strength and the transmission delay, this configuration exhibits various fixed point attractors, and limit cycles occur for delays greater than half the period of an uncoupled unit. (We consider the one-dimensional state space that is defined by the temporal interval between the spike emission of the two units.[2]) Although analytical descriptions for selected parameter ranges appear tractable, a rigorous *and* compact mathematical formulation of the *general case* is out of reach. However, the desynchronizing influence of transmission delays for excitatory coupling is confirmed by computer simulations of 'two unit' systems (Kirillov and Woodward 1993) as well as of larger and more realistic model networks with local interconnections (Nischwitz et al. 1991, 1992). Synchronization is reported to reappear for delays that are approximately multiples of the interspike interval of an uncoupled unit (Gerstner and van Hemmen 1992; Glünder and Nischwitz 1993).

2.4 Inhibitory coupling without transmission delay

The effect of inhibitory interconnections without delay can be studied from the example in Fig. 1e, where we again use the initial condition of Fig. 1c. The first impulse from unit 1 delays the triggering of an impulse by unit 2 (positive time shift Δt_2) whereas the spike returned by unit 2 causes a less delayed $\Delta t_1 < \Delta t_2$ impulse emission by unit 1 and therefore the spike events diverge temporally. As with the previously described configuration (Fig. 1c) the synchronous state is repellent and impulse emission in counterphase is attractive. Mirollo and Strogatz (1990), who treat this inhibitory case as well, prove – again for units without a refractory period – the attraction of the counterphase situation. For units with a refractory interval it can additionally be shown that the synchronous state is repellent and that further fixed points cannot occur.

2.5 Inhibitory coupling with transmission delay

Finally, the behaviour of delayed ($\vartheta = 4$ ms) inhibitory coupling – the condition we are most interested in – is exemplified in Fig. 1f. Again, we apply the initial condition from Fig. 1c, e. The first impulse emitted by unit 1 arrives at unit 2 after this unit has fired itself. Hence, the somatic potential $u_2(t)$ of unit 2 is low when it receives the inhibitory input and the resulting positive time shift Δt_2 is smaller than the one caused by the subsequent inhibition of unit 1 ($\Delta t_1 > \Delta t_2$). Consequently, the asynchrony

[2] This definition is well suited for formulations of the so-called stroboscopic or return map.

between the units becomes smaller. As with the non-delayed excitatory system (Fig. 1b), the synchronous state is attractive but, in contrast to the non-delayed excitatory system, the counterphase state – if it exists – is also attractive. For the parameter setting in our example, the counterphase state does not exist. It occurs if unit 2 does not fire before it receives input from unit 1 and vice versa, a situation that depends on the initial asynchrony and requires smaller coupling strengths or delays than those used in our example. Similar to the delayed excitatory configuration, limit cycles join the fixed point attractors for transmission delays larger than half the firing period of an uncoupled unit but, in contrast to the excitatory case, limit cycles occur for small delays as well. Hence, again one encounters problems with a compact analytical formulation of the general case that covers the whole manifold of attractors as a function of coupling strength and delay. Again, simulations performed by Kirillov and Woodward (1993) confirm the synchronizing influence of transmission delays and the importance of the initial asynchrony for 'two unit' systems with inhibitory interconnections. Owing to the interesting and biologically relevant properties of this coupling scheme (see Sect. 5), we devote this article to the description of phenomena in large and more realistic model networks with local interconnections.

2.6 Time course of synchronization

Two of the four basic configurations can produce stable synchrony although their synchronization behaviour is quite different. In the case of non-delayed excitatory coupling the efficacy of the synchronization process increases with increasing synchrony. This is because the difference of the time shifts $|\Delta t_1 - \Delta t_2|$ increases with synchrony until the units' states are similar enough to be exactly synchronized by a single impulse. Consequently, synchronization increases slowly initially and quickly converges to perfect synchrony. In the case of delayed inhibition, the efficacy of the synchronization process decreases with increasing synchrony because the difference of the time shifts $|\Delta t_1 - \Delta t_2|$ decreases with increasing synchrony. This means that a moderate and stable level of synchronization is attained after a very few interactions but that perfect synchrony occurs either never or under favourable conditions, i.e. in general by chance.

Clearly, the minimalistic 'two unit' system allows a basic understanding and analytical insights[3] into the performance of coupled formal neurons. However, here we are interested in the behaviour of more natural systems, especially those with local inhibitory and delayed interconnections. We must therefore consider more refined formal neurons in larger networks; these are introduced in the following section.

[3] A detailed mathematical treatment of the 'two unit' system, including a fixed point analysis of the dynamics and the corresponding basins of attraction, is given in Nischwitz (1994).

3 Model network with local lateral inhibition

For our investigations we needed an input-controlled and impulse-generating formal neuron with refractory period that is still computationally manageable in populations of more than 50 units and in simulations with high temporal resolution ($\delta t \ll 1\,\text{ms}$). We decided to simulate 'leaky integrate and fire' units that are related to the hardware neuromime proposed by French and Stein (1970). A chain of such formal neurons that are reciprocally interconnected by inhibitory weighted local links of adjustable transmission delay was considered as the network architecture.

3.1 Model neuron

Our model neuron has a subthreshold behaviour of a leaky integrator that is characterized by its δ-impulse response

$$h(t) = e^{-t/\tau}/\tau \quad \text{for } t \geqslant 0$$

where the time constant $\tau = 10\,\text{ms}$. We distinguish three kinds of input signals that are linearly summed by every unit, i.e. we consider neither nonlinear synaptic transmission or interaction, nor any nonlinear dendritic conduction (but see Sect. 5.4). (All potentials are normalized to the threshold voltage θ.)

The excitatory feeding input $e(t)$ represents stimulations from outside the network and changes the somatic potential by $u_e(t) = e(t) \ast h(t)$, where '$\ast$' denotes convolution. For most of the investigations reported here, we assume a constant feeding input $E := e(t) = const.$ for times $t \geqslant 0$ that simulates incoherent activity at many weakly transmitting, e.g. 'apical dendritic' synapses (Fig. 4) and that changes the somatic potential according to the step response (Fig. 3)

$$u_E(t) = E\left(1 - e^{-t/\tau}\right) \quad \text{for } t \geqslant 0\,.$$

The lateral inhibitory input $a(t) = \sum_\nu w_\nu \cdot p_\nu(t - \vartheta)$ is the weighted sum of impulse trains $p_\nu(t) = \sum_\kappa s(t - t_{\kappa\nu})$ that are transmitted with delay $\vartheta = const.$ and $w_\nu < 0$ from ν neighbouring units via, for example 'basal dendritic' or 'somatic' synapses, i.e. from inside the network (Fig. 4). (The variable $t_{\kappa\nu}$ indicates the temporal position of the κ^{th} action potential in the ν^{th} impulse train.) This lateral inhibition alters the somatic potential according to $u_a(t) = a(t) \ast h(t)$. We do not consider synaptic habituation or any other temporal changes of the synaptic transmission. Figure 2 shows the assumed exponentially decaying action potential $s(t)$ with $\tau_{AP} = 0.144\,\text{ms}$ together with its postsynaptic response $u_{PSP}(t)$ that is normalized to its coupling strength w. Referring to van Vreeswijk et al. (1994) this response must be termed fast rising. The noise input $n(t)$ is a random process with uniformly distributed amplitudes from the range $\pm E/2$ and mimicks stochastic fluctuations $u_n(t) = n(t) \ast h(t)$ of the somatic potential. This input component is individually computed for each model neuron.

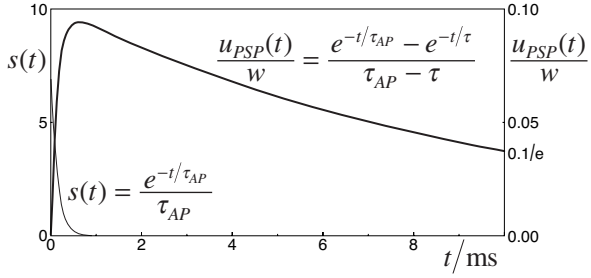

Fig. 2. Action potential (spike) $s(t)$ and normalized postsynaptic potential $u_{PSP}(t)/w$

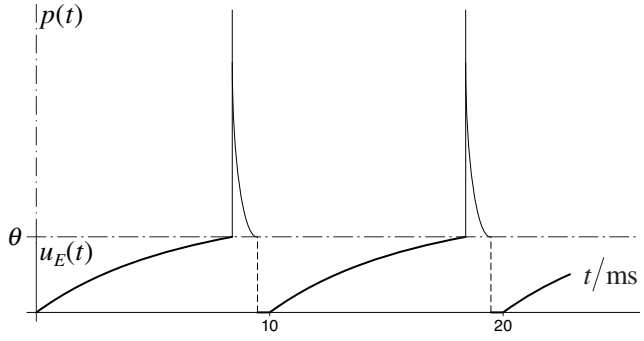

Fig. 3. Typical time course of the noiseless subthreshold somatic potential $u_E(t)$ and of the generated spike train $p(t)$ with the interspike interval $T_w(E) = 10\,\text{ms}$

In total, the change of the subthreshold somatic potential from the resting potential is given by

$$u(t) = u_e(t) + u_a(t) + u_n(t) = [e(t) + a(t) + n(t)] \ast h(t)$$

When this potential exceeds the threshold θ, then an action potential $s(t)$ is triggered and 1 ms later $u(t)$ is set to the refractory potential for a period of 0.5 ms before the integration can start again (Fig. 3). The feeding input E is specified by the period T_0 of the impulse train it evokes in a single noise-free unit.

3.2 Network

Figure 4 depicts the neighbourhood of a model neuron in the proposed one-dimensional single stage network. In order to avoid boundary problems in networks of manageable size, the chain is cyclically closed and all its N units are coupled in the same way. We consider local inhibitory interconnections without direct feedback from units onto themselves. Every unit receives input from its immediate $k \ll N$ neighbours on either side with an absolute strength $|w_\nu|$ that decreases linearly with the distance, i.e. with $|\nu|$. Unlike the coupling strength, the transmission delay ϑ is assumed constant, which implies similar axonal conduction times as well as synaptic and postsynaptic processing [see Glünder and Nischwitz (1993) for a discussion of this assumption with respect to conjectures about the functional relevance of spike synchronization]. In order to characterize the efficacy of interaction in the network, we introduce the total coupling

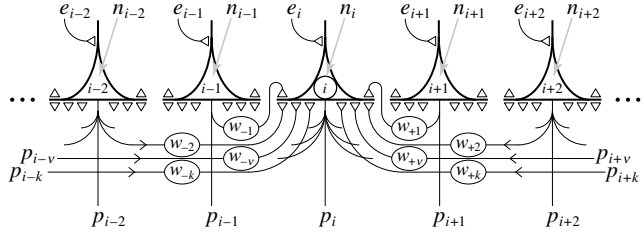

Fig. 4. Local interconnection scheme of a unit in the one-dimensional network

strength

$$W = \sum_{\substack{\nu=-k \\ \nu\neq 0}}^{+k} w_\nu = const.$$

of every unit. Using the definitions of the preceding subsection a *single* input spike triggers a spike in the target unit for coupling strengths $w \geqslant 10.65$. With excitatory coupling care has to be taken not to exceed a critical coupling strength at which externally unstimulated units are activated, for instance by synchronous unilateral input, and that would result in the stimulus-independent synchronization of the whole population. No such limit exists for the inhibitory coupling considered here because in our simulations the somatic potential cannot drop below the refractory value.[4]

3.3 Network simulation and measures of synchrony

We studied the *discrete* nonlinear dynamics of the network, i.e. we performed simulations on a digital computer with the temporal resolution δt. Because temporally discrete simulations can cause severe problems with system descriptions that do not satisfy the Lipschitz condition – such as the system considered here – we were very cautious of interpreting our results (see Sect. 5.4). As a further consequence of such simulations, a zero delay in the lateral links can only be approximated, i.e. we must accept the mean intrinsic delay of $\vartheta_0 = \delta t/2$. For the experiments reported here, all units of the network received the same feeding input for times $t \geqslant 0$. However, their initial somatic potentials ($t < 0$) were individually set to uniformly distributed random potentials from the 'refractory potential to threshold' range. This initiation was carried out afresh for each run of the simulation. Unless stated otherwise, the values for the network parameters were chosen as follows:

$\delta t_S = 0.1\,\text{ms}$; $N_S = 64$; $k_S = 8$;

E_S so that $T_0 = 10.7\,\text{ms}$

This standard setting was found to be useful for most of our investigations and does not represent an extreme

[4] In previous publications we referred the coupling strengths to the critical coupling strength. Owing to its irrelevance for inhibitory interconnections we decided here to use the actual values. They result from multiplying the previous values by 16.

choice. The influence of deviations from these standard values on the quality of synchronization is dealt with elsewhere (Nischwitz et al. 1991; Kraut et al. 1993).

In order to quantify the degree of synchronization, we define the instantaneous spike density

$$S(t) = \tfrac{1}{NM} \sum_{i=1}^{N} \sum_{j=0}^{M-1} P_i(t - j\delta t)$$

that can be imagined as a slightly lowpass-filtered recording of the whole spiking activity to which all units contribute with the same strength (cf. Figs. 6 and 7). It computes as the binarized spike activity

$$P_i(t) = \begin{cases} 1 & \text{for } (t - t_{\kappa i}) < M \cdot \delta t \text{ for } t_{\kappa i} \leqslant t \\ 0 & \text{else} \end{cases}$$

in a spatio-temporal window that is N units long and one spike duration $M \cdot \delta t = 1\,\text{ms}$ wide, divided by the maximum possible activity in this window.[5] Consequently, $S(t) = 1$ denotes an instant of perfect synchrony, i.e. all N units must have *triggered* action potentials at exactly the same time. From the spike density we derive the quality factor of synchronization

$$\eta_{200} = \tfrac{1}{50} \sum_{\mu=1}^{50} \max_{150 < t \leqslant 200\,\text{ms}} \{S_\mu(t)\}$$

which is the mean over 50 runs of the maximum spike densities in the temporal interval 150…200 ms. For an assessment of the quality factor we provide the reference quality $\eta_{\text{ref}}(r)$ that results from 'synchrony by chance' in the uncoupled ensemble and which is a strictly monotonous function of the impulse rate $r(W = 0)$. Hence, we obtain the reference quality for coupled networks by using the observed impulse rates $r(W)$.

4 Simulation results

In Figs. 5 and 6 we present a compilation of the essential results from our simulations of inhibitory and noisy '64-unit' systems. We show two groups according to their feeding input $E = E_S$ (Fig. 5a, b and Fig. 6a, b) and $E = 1.85\,E_S$ (Fig. 5c, d and Fig. 6c, d).

4.1 General

A first qualitative inspection of the graphs in Fig. 5a, c confirms the behaviour predicted from the corresponding 'two unit' systems in the Sects. 2.4 and 2.5. (The evaluated quality factors are interpolated for better display.) For the minimum delay $\vartheta_0 = 0.05\,\text{ms}$ (open circles) desynchronization ($\eta_{200} < \eta_{\text{ref}}$) is obvious for the investigated coupling strengths W and stimulations E. A significant transmission delay of $\vartheta = 4.05\,\text{ms}$ (open diamonds) leads to an increase in synchrony with increasing coupling strength $|W|$ until it saturates at values $\eta_{200}(E_S, W = -16) \approx 0.6$ and $\eta_{200}(1.85\,E_S, W = -11) \approx 0.8$. The superior synchrony for the higher feeding input is essentially due to two effects. Firstly, the shorter mean interspike interval of $T_{-22}(1.85\,E_S) \approx 9\,\text{ms}$ versus $T_{-22}(E_S) \approx 15\,\text{ms}$ results in less accumulation of noise and thus in a smaller standard deviation of the somatic potential. Secondly, the slope of the somatic potential at the threshold is steeper which makes the conversion of voltage noise to impulse jitter less effective.

The bold curves in Fig. 5b, d depict the synchronization quality as a function of the transmission delay. Especially for strong stimulations, the quality factor remains at a high level over a wide range of delays, except for dips around transmission delays that are approximately multiples of the period of the uncoupled unit $T_0(1.85\,E_S) \approx 5.5\,\text{ms}$, or $T_0(E_S) \approx 10.7\,\text{ms}$ respectively. The dashed curves show the corresponding reference qualities that reflect the spike rates. In order to understand the pronounced sawtooth-shaped graph in Fig. 5d, we consider two particular system states. For very small transmission delays (here: $\vartheta \leqslant 0.5\,\text{ms}$) the network produces asynchronous or even desynchronized activity (cf. Fig. 6d) and thus, on average, the units are fairly depolarized when they receive inhibitory impulses. Consequently, the subsequent impulse emission is considerably delayed which results in a low mean firing rate [in Fig. 6d: $T_{-22}(1.85\,E_S, \vartheta_0) \approx 13.5\,\text{ms}$]. Conversely, the highest mean rate must be expected for minimally delayed impulse emission that takes place if the units receive impulses during their refractory period. Obviously, this state can only occur in cases of excellent synchrony. Actually, in our noisy system it is not observed for the theoretically expected transmission delays, i.e. for multiples of the period of an uncoupled unit $T_0(E)$ (here: 5.5 ms, 11 ms etc.), but for greater transmission delays (here: 7 ms, 12.5 ms etc.). The main reason for this is advanced firing caused by imperfect synchrony (noise). Under the condition considered here, advanced firing produces the largest possible delays in the impulse emission of the receiving units and thus leads to destructive interference (Glünder and Nischwitz 1994). This in turn results in low spike rates and shows up as dips in the synchronization quality (e.g. indicated by the double arrow head in Fig. 5d).

We shall now focus on details of our simulation results that require more detailed signal representations as well, namely spike density plots and displays of spatio-temporal spike patterns. In contrast to the graphs in Fig. 5, they display data from individual runs. For convenience we indicate (by arrows in Fig. 5) the quality factors to which these individual data contribute.

4.2 Synchronization (delayed transmission)

Here we consider the constant transmission delay $\vartheta = 4.05\,\text{ms}$ and discuss phenomena that arise from variations of the coupling strength and of the feeding input. Figure 6a (top) represents a typical time course of the instantaneous spike density for the standard stimulation

[5] The running temporal average is causally computed. Consequently, the spike densities appear slightly shifted (later) when compared with the corresponding spike patterns (Fig. 6).

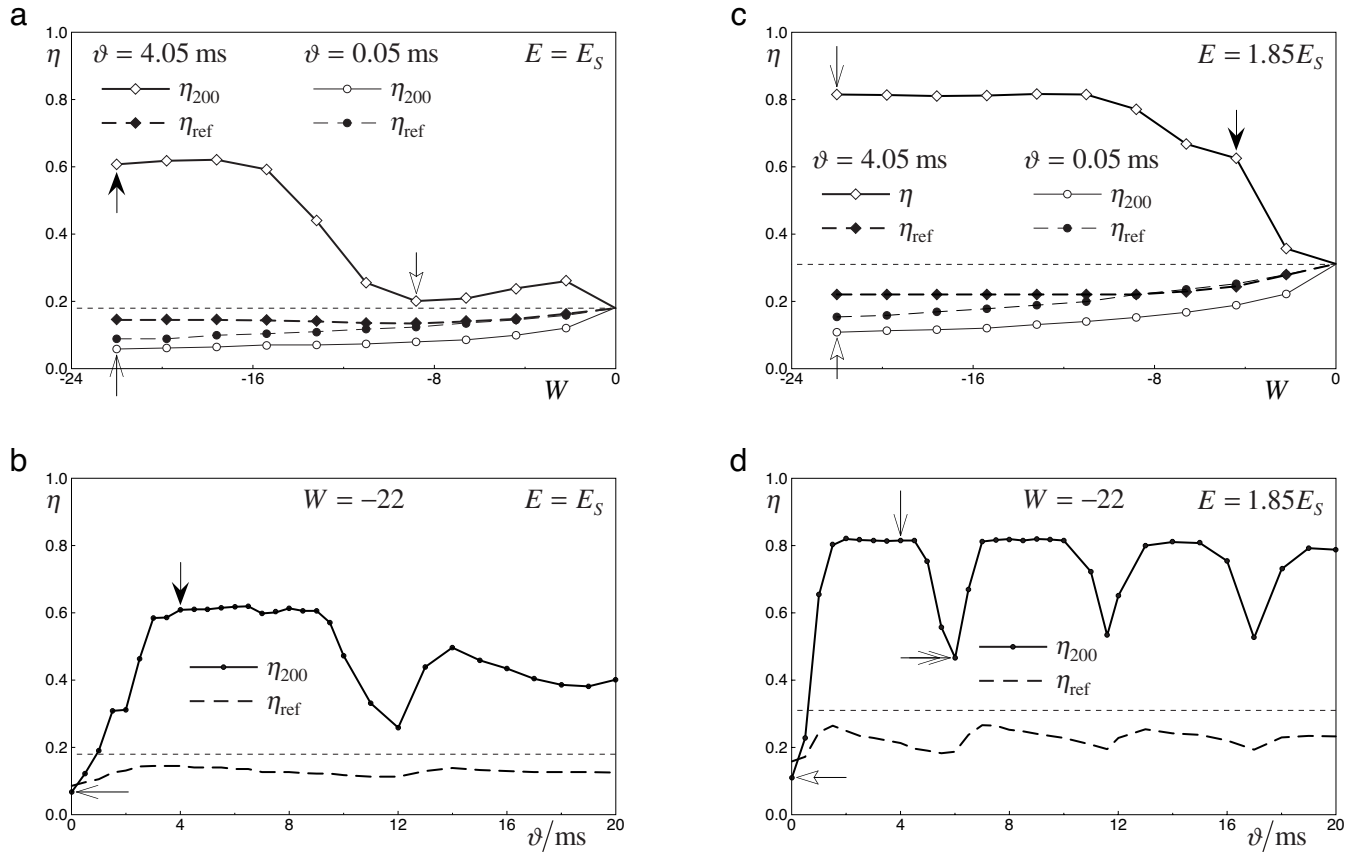

Fig. 5a–d. Mean synchronization qualities η for various parameter settings of the noisy network with lateral inhibition. **a**, **c** Synchronization η_{200} – 150 ms after onset – as a function of coupling strength W and for two delay times ϑ as well as for two feeding inputs E. The reference quality η_{ref} indicates the 'synchrony by chance'. **b**, **d** Synchronization η_{200} as a function of transmission delay ϑ for the same two stimulations. (*Arrows* indicate corresponding parameter settings and those used for the results shown in Fig. 6.) For further details see the text

with *strong coupling* $W < -12$. After typically two interactions (20…50 ms), the majority[6] of such simulation runs lead to a comparatively stable and synchronous network state. During the first about 15 ms of the corresponding spike pattern [Fig. 6a (bottom)] we observe that less than half the units reach the threshold and that they fire exclusively within the first 4.5 ms. This is surprising because the initial somatic potentials are uniformly distributed in the 'refractory potential to threshold' range. Hence, we must conclude that a very few early firing units suffice to suppress the triggering of the remaining units at times after the earliest spikes become effective ($\vartheta = 4.05$ ms). Consequently, this phenomenon must be attributed to the highly effective inhibitory coupling.

Spatio-temporal clustering is observed for the standard stimulation and *low coupling* strengths ($-12 < W < 0$). Figure 6b shows a typical example with two or three moderately synchronous clusters that emerge after about 100 ms and vary slowly in size and phase (note the different time scale). Despite noise, global synchrony is maintained if the units have sufficiently similar start depolarizations. Comparable to the corresponding 'two unit' system (Sect. 2.5) the final spike pattern depends on the initial asynchronies: if all units fire before the first spikes become effective, synchrony is established; otherwise spatial clustering occurs. Note also that the appearance of such clustered spike patterns is essentially independent of the size of the population and that clustering happens in open chains as well. The risk of misleading interpretations of MUA recordings, especially with respect to period doubling and so-called spindles, is exemplified by use of this system state in Glünder and Nischwitz (1994).

More intense stimulation, i.e. $E = 1.85 E_S$, leads to synchrony for all the investigated start conditions as long as the coupling strength suffices to overcome the disturbing influence of the noise (here: $W \approx -4.4$). Figure 6c shows a typical result with the rapid initial increase in synchrony and the slow approach towards the maximum value. In contrast to the spike pattern of Fig. 6a, the conspicuous temporal concentration during the first milliseconds is not observed: owing to the shorter interspike interval – which is in the order of the transmission delay – most of the units emit a spike before they receive their first impulses.

[6] As a consequence of our ring-shaped network (closed chain), about 2% of the runs lead to circulating, i.e. spatio-temporally inclined spike fronts. This means that impulses of neighbouring units have an average temporal offset of T_W/N.

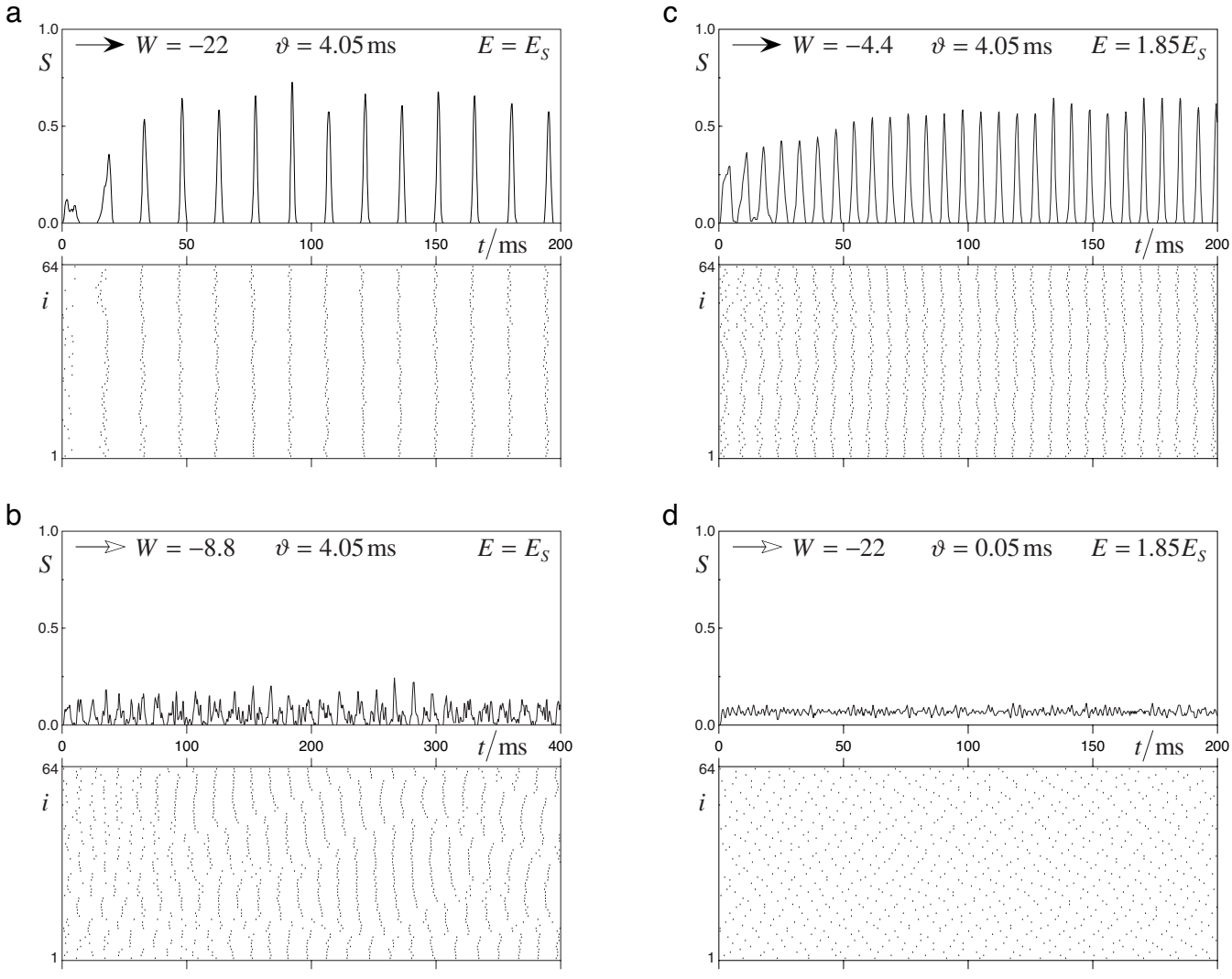

Fig. 6a–d. Individual data for selected parameter settings: spike density plots (*upper parts*) and corresponding spatio-temporal spike patterns with *dots* indicating spikes (*lower parts*): **a** for strong coupling with delay and standard stimulation; **b** as for **a** but for weak coupling that produces clustering; **c** for very weak coupling and higher stimulation; **d** for strong coupling, minimum delay and higher stimulation that leads to desynchronization

4.3 Desynchronization (*non-delayed transmission*)

It can be seen from Fig. 5b, d that desynchronization ($\eta_{200} < \eta_{\text{ref}}$) occurs only in networks with minimum delay $\vartheta_0 = 0.05\,\text{ms}$. Evidently, our definition of desynchronization means that the spike pattern has a higher degree of order than the spatio-temporal output of the uncoupled population. This asynchronous but orderly state is apparent in the spike pattern of Fig. 6d with its evenly distributed impulses in space and time. Again, this behaviour parallels that of the corresponding 'two unit' system (Sect. 2.4) with its attractive counterphase state: the system tends to maximize the spatio-temporal distances between adjacent spikes.

4.4 Time-varying stimulation

The data in Fig. 7a, b demonstrate the response of the standard network with *strong coupling* $W = -22$ and delay $\vartheta = 4.05\,\text{ms}$ to temporally changing stimuli and thus its ability to produce aperiodic spike fronts. The linear downward sweep of the feeding input $E(t) = (1.85 - 3.375 \cdot t/[s])\,E_S$ results in a nonlinear decrease of the spike rate. Figure 7a shows that the synchrony remains constant on a high level down to $E(200\,\text{ms}) \approx 1.2\,E_S$ and declines for smaller stimulations until the activity vanishes for $E(t > 370\,\text{ms}) < 0.6\,E_S$. Comparable results are obtained in networks with excitatory interconnections (Glünder and Nischwitz 1993). Even more impressive is the immediate reaction to abrupt changes of the feeding input. Figure 7b shows well-synchronized spike fronts whose rate rapidly follows the 10 Hz square wave stimulation that switches between $E_{\max} = 1.85\,E_S$ and $E_{\min} = E_S$. Although synchrony generally decreases for reduced stimulations, synchrony once established is not severely disturbed even by dramatic changes in the feeding input. Synchrony does not signifi-

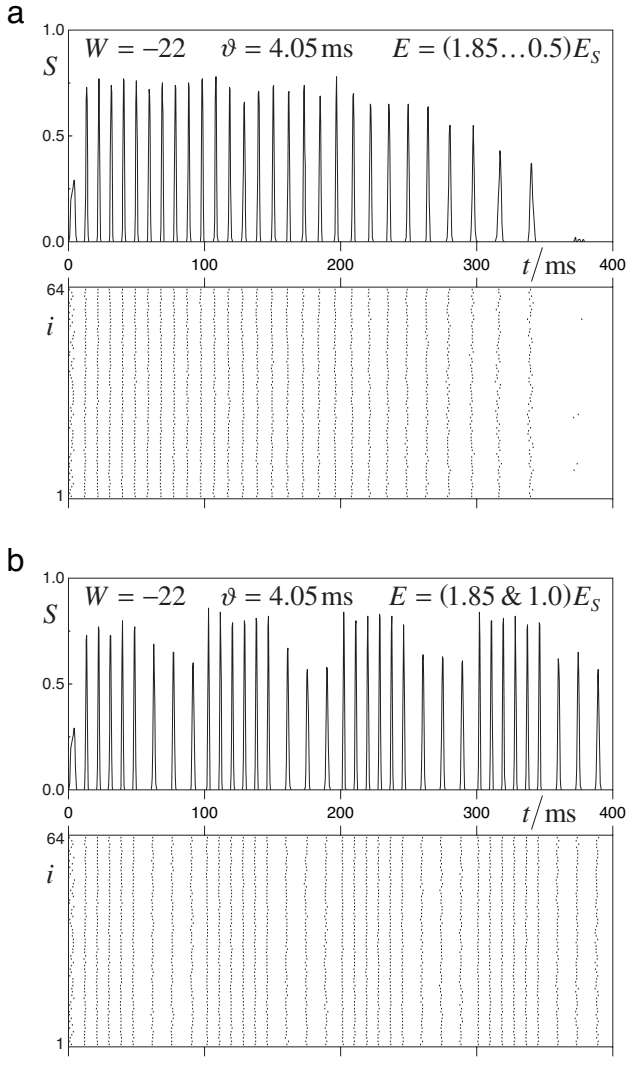

Fig. 7a, **b.** Spike density plots and corresponding spike patterns: **a** for a linearly decreasing stimulation; **b** for a 10 Hz square wave stimulation

cantly differ from that obtained with the corresponding constant feeding. For $E = E_S$ this can be verified by comparing the spike densities in Fig. 6a with those in Fig. 7a for $t \approx 250$ ms and those in Fig. 7b during the periods of low stimulation.

Moreover, these simulation results are good examples of the feasibility of synchronized aperiodic activity, i.e. of aperiodic spike fronts. Data from simulations with *spatially* changing stimuli in networks with excitatory interconnections have been reported elsewhere (Nischwitz et al. 1992).

5 Discussion

Our investigations of externally driven populations of locally interconnected and noisy 'leaky integrate and fire' model neurons show that substantial inhibition and non-vanishing delay in the lateral links lead to highly synchronous impulse emission that is maintained under temporally varying stimulations. Weak lateral inhibition can produce time-varying clusters of synchronized units and very small delay results in desynchronization. Again, we emphasize that coupling strength and delay determine the system's behaviour to a comparable extent. Throughout the discussion we substantiate our claim that – given a biologically reasonable choice of delay and coupling strength – *delayed local inhibition* is currently the most convenient scheme for spike synchronization. This view recently received additional support for another reason (van Vreeswijk et al. 1994).

For the following reasons we shall not directly relate our work to investigations that deal with networks of coupled non-spiking oscillators:

- Spike synchronization may lead to recordings of neural group activity with quasi-periodic components. However, the synchronization process itself is unlikely to be based on such signals.
- Impulse-coupled 'leaky integrate and fire' units behave essentially differently from continuously coupled oscillators. Although Kuramoto (1991) tried to unify the two approaches he could not be successful in every respect (for an example see Sect. 5.2). His crucial assumption of fully interconnected networks with infinitely many units $N \to \infty$ necessitates vanishing coupling $W \to 0$ to maintain the finite input to each of them. Thus, in the limit, the loss of what makes the coupling discontinuous is evident!
- Networks of 'leaky integrate and fire' units are externally driven and generate stimulus-dependent spike rates. They therefore differ from most of the oscillator networks that essentially remain locked to frequencies in the γ-band.

With this functionally founded restriction, our investigations remain to be compared with work that deals with synchronization by inhibitory as well as excitatory impulse coupling.

5.1 Lateral and central inhibition

The work closest to ours is that of Kirillov and Woodward (1993, section 3.1), whose results from simulations of the 'two unit' system with inhibitory and delayed links nicely confirm our considerations in Sect. 2. As already mentioned, this minimalistic system allows one to study basic principles but it is not sufficient for an evaluation of the various states exhibited by larger populations. The authors' interesting finding of a noise-induced temporal switching between synchrony and counterphase does not show up in our simulations (except perhaps for some units and epochs with destructive interference; see the end of Sect. 4.1) that may either be due to a different noise level or to the network size. Quite different is the synchronization scheme investigated by Lytton and Sejnowski (1991; Sejnowski and Lytton 1992) with two externally stimulated formal neurons receiving a common periodic inhibitory signal. This results in a unidirectional flow of the synchronization signal in contrast to networks with distributed cooperative or competitive interactions.

5.2 Lateral excitation

Simulations of excitatorily coupled networks with small or minimum transmission delay, either fully (Deppisch et al. 1992) or locally (MacGregor and Palasek 1974; Hartmann and Drüe 1990) interconnected, exhibit spike synchronization. For fully connected networks *without delay* Mirollo and Strogatz (1990) even managed to prove the global stability of the synchronous state. On the basis of this work, Kuramoto (1991) tried a unified analytical description of continuously and impulse coupled networks, and applied it to fully connected networks with delay and noise. His conclusions agree with results from investigations of non-spiking oscillator networks with excitatory and delayed interconnections (Schuster and Wagner 1989; Niebur et al. 1991) that reveal synchronization up to delays of a quarter of the interspike interval. In pronounced contrast to these findings theoretical analyses (Nischwitz 1994) and simulations (Kirillov and Woodward 1993, section 3.2; Nischwitz and Glünder 1993) of impulse-coupled 'two unit' systems as well as simulations of fully connected (Gerstner and van Hemmen 1992) and of locally impulse coupled (Nischwitz et al. 1991, 1992; Glünder and Nischwitz 1993) populations reveal a rapid decline in synchrony with increasing delay. For our formal neuron, synchronization is down at the reference level for transmission delays $\vartheta \geqslant 1\,\mathrm{ms}$, except around multiples of the period of an uncoupled unit. Because these peaks widen with the coupling strength, increased excitatory coupling is a common remedy for decreasing synchronization quality, especially in networks with small transmission delay that is most often due to a coarse temporal resolution δt of the computer simulation (cf. Sects. 3.3 and 5.4). Different from lateral inhibition, where excessive coupling causes any activity to cease, care must be taken not to exceed the critical excitatory coupling at which externally unstimulated units are excited by lateral input (see Sect. 3.2) and that leads to the pathological state of stimulus-independent activation of the whole network.

5.3 Lateral excitation with additional inhibition

Investigations of a layered population of excitatorily coupled 'leaky integrate and fire' model neurons that strongly interact with inhibitory interneurons are of considerable biological relevance.[7] Regarding synchronization, the role of inhibition in recently investigated types of networks essentially differs from that in our approach. For the network thoroughly considered by Gerstner et al. (1993a, b) its main purpose is the above-mentioned control of activity in otherwise excitatorily synchronized networks. Thus, and with respect to the relation of transmission delay to interspike interval, their results agree well with those obtained from purely excitatorily coupled networks (Nischwitz et al. 1991; Gerstner and van Hemmen 1992). In the model proposed by Bush and Douglas (1991) synchronization is achieved by a central inhibitory control that gates the activity of all excitatorily coupled units. It should be noted that the behaviour of such schemes is rather restricted. For instance, within a controlled region they will hardly produce stimulus-dependent subpopulations (Nischwitz et al. 1992) or synchronized clusters such as those shown in Fig. 6b.

5.4 Simulation technique and refinements

We showed results from computer simulations with the temporal resolution $\delta t_S = 0.1\,\mathrm{ms}$, while most authors use larger increments such as $\delta t = 0.5\,\mathrm{ms}$ (Deppisch et al. 1992; Gerstner and van Hemmen 1992) or even $\delta t = 1\,\mathrm{ms}$ (MacGregor and Palasek 1974; Hartmann and Drüe 1990). Owing to the situation mentioned in Sect. 3.3, we were interested in the influence of the resolution on the results and thus we performed most of the simulations with various and up to 100 times smaller increments. For all of the parameter settings investigated, we found that the quality factor η_{200} – the mean over 50 differently initialized runs – remained essentially unaffected for increments $\delta t \leqslant 0.1\,\mathrm{ms}$ but in a few cases the dynamics of single runs and thus the corresponding spike densities varied considerably with the temporal resolution (Kraut et al. 1993; Nischwitz 1994). We took care not to present unreliable results of this sort. Although cases are known in nonlinear dynamics where increasing temporal resolution does *not* lead to the convergence of the behaviour of a discrete system towards that of its continuous version or original (Wang and Blum 1992), we recently revealed (Nischwitz 1994) by using a piecewise continuous method that our discretely simulated system does indeed convergently approximate the behaviour shown by the corresponding piecewise continuous simulations.

We demonstrated that synchrony up to fractions of the impulse duration can be obtained with simple formal neurons and biologically plausible network parameters. Neither additional nonlinearities, such as multiplying synapses (Eckhorn et al. 1990) or so-called NMDA synapses (Kirillov and Woodward 1993), compartmental modelling (Bush and Douglas 1991; Sejnowski and Lytton 1992), nor different time constants for feeding and lateral inputs (Hartmann and Drüe 1990), are required for good spike synchronization. Nevertheless, a positive effect on the synchronization behaviour of inhibitorily coupled networks is expected if the synaptic transmission is more realistically implemented: The conductance change at the postsynaptic membrane – a parametric change of the electrical circuit – means a moderately nonlinear transmission (Rall 1964) that, compared with the commonly assumed linear current input, produces a slight decrease/increase in the amplitude of excitatory/inhibitory postsynaptic potentials with increasing depolarization. Therefore, this effect influences the somatic integration characteristic and thus impulse synchronization: lateral inhibition is favourable, lateral excitation adverse. Furthermore, the analysis by van Vreeswijk et al. (1994) of the *non-delayed* 'two unit'

[7] Although our knowledge about excitatory/inhibitory interactions – preferably in neocortex – still allows for a wide variety of network types, we are presently investigating functionally defined interconnection schemes (Glünder and Antesberger 1995).

system with more general postsynaptic responses reveals that "if the rise time of the synapse is longer than an action potential, inhibition not excitation leads to synchronized firing".

We used higher spike rates than generally reported or observed in electrophysiological experiments. However, this is irrelevant in the context of our synchronization scheme since it principally functions over a wide range of stimulus-dependent rates (cf. Fig. 7). This feature makes our network different from most schemes of coupled oscillators. Moreover, recent results from investigations of the visual cortex of an awake monkey reveal strong stimulus-dependent changing(!) high-frequency components of up to 100 Hz in neural group activity (Eckhorn et al. 1993).

5.5 Neurobiological aspects

Great support for the local lateral inhibition scheme comes from neuroanatomy: in the neocortex (inhibitory) stellate cells act strictly locally (typical connectivity diameter 250 μm) and highly effectively on the surrounding (excitatory) pyramidal cells that are the main information processing units and that make long-range interconnections (Braitenberg and Schüz 1991, chapters 15 and 35). Moreover, the inhibitory input to pyramidal cells is estimated to be up to 100 times more effective than the excitatory one (Sejnowski and Lytton 1992), a fact that is not in favour of spike synchronization by excitatory links. Monosynaptic impulse transmission between neighbouring neurons (axon hillock to soma) must be assumed to require $\vartheta_{\mathrm{exc}} > 1\,\mathrm{ms}$, which is fairly prohibitive for good and stimulus-specific synchronization by lateral excitation (except for the mentioned peaks: Sect. 5.2). Of course, inhibitory coupling must involve inhibitory interneurons that make the impulse transmission disynaptic with $\vartheta_{\mathrm{inh}} > 2\,\mathrm{ms}$. This lower boundary fits nicely with the first plateau of good synchronization by lateral inhibition shown in Fig. 5d. Finally, synchronization of neurons with slowly rising postsynaptic potentials seems to require inhibitory neural coupling (van Vreeswijk et al. 1994).

Interestingly, there is evidence for inhibitory impulse synchronization in a completely different biological system, namely the synchronous emission of light flashes in populations of certain species of fireflies. Buck (1988) proposes a model with delayed and strong inhibitory links between these comparably complex 'units'.

Acknowledgements. We thank J. L. van Hemmen for encouraging us to compile our results and for supplying an elegant formulation. Most of the investigations were performed while H. G. was supported by the 'Volkswagen-Stiftung' under grant I/65 914.

References

Adrian ED (1935) The electrical activity of the cortex. Proc R Soc Med 29:197-200

Atiya A, Baldi P (1989) Oscillations and synchronizations in neural networks: an exploration of the labeling hypothesis. Int J Neural Syst 1:103–124

Braitenberg V, Schüz A (1991) Anatomy of the cortex: statistics and geometry. Springer, Berlin Heidelberg New York

Buck J (1988) Synchronous rhythmic flashing of fireflies. II. Q Rev Biol 63:265–289

Bush PC, Douglas RJ (1991) Synchronization of bursting action potential discharge in a model network of neocortical neurons. Neural Comput 3:19–30

Cairns DE, Baddeley RJ, Smith LS (1993) Constraints on synchronizing oscillator networks. Neural Comput 5:260–266

Coultrip R, Granger R, Lynch G (1992) A cortical model of winner-take-all competition via lateral inhibition. Neural Networks 5:47–54

Deppisch J, Bauer H-U, Schillen T, König P, Pawelzik K, Geisel T (1992) Stochastic and oscillatory burst activities in a model of spiking neurons. In: Aleksander I, Taylor J (eds) Artificial neural networks 2. Elsevier, Amsterdam, pp 921–924

Eckhorn R, Bauer R, Jordan W, Brosch M, Kruse W, Munk M, Reitboeck HJ (1988) Coherent oscillations: a mechanism of feature linking in the visual cortex? Biol Cybern 60:121–130

Eckhorn R, Reitboeck HJ, Arndt M, Dicke P (1990) Feature linking via synchronization among distributed assemblies: simulations of results from cat visual cortex. Neural Comput 2:293–307

Eckhorn R, Frien A, Bauer R, Woelbern T, Kehr H (1993) High frequency (60-90 Hz) oscillations in primary visual cortex of awake monkey. Neuroreport 4:243–246

Engel AK, König P, Gray CM, Singer W (1990) Stimulus-dependent neuronal oscillations in cat visual cortex: inter-columnar interaction as determined by cross-correlation analysis. Eur J Neurosci 2:588–606

Engel AK, König P, Singer W (1991) Direct physiological evidence for scene segmentation by temporal coding. Proc Natl Acad Sci USA 88:9136–9140

Engel AK, König P, Singer W (1993) Bildung repräsentationaler Zustände im Gehirn. Spektrum Wiss, no 9:42–47

Freeman WJ (1975) Mass action in the nervous system. Academic Press, New York

French AS, Stein RB (1970) A flexible neural analog using integrated circuits. IEEE Trans Biomed Eng 17:248–253

Gerstner W, Hemmen JL van (1992) Associative memory in a network of 'spiking' neurons. Network 3:139–164

Gerstner W, Ritz R, Hemmen JL van (1993a) A biologically motivated and analytically soluble model of collective oscillations in the cortex: I. Theory of weak locking. Biol Cybern 68:363–374

Gerstner W, Ritz R, Hemmen JL van (1993b) Why spikes? Hebbian learning and retrieval of time-resolved excitation patterns. Biol Cybern 69:503–515

Glünder H, Antesberger M (1995) Same network – different formal neurons. Two network implementations for competitive motion analysis. In: Elsner N, Menzel R (eds) Learning and memory. Göttingen Neurobiology Report 1995. Thieme, Stuttgart, p 895

Glünder H, Nischwitz A (1993) On spike synchronization. In: Aertsen A (ed) Brain theory. Spatio-temporal aspects of brain function. Elsevier, Amsterdam, pp 251–258

Glünder H, Nischwitz A (1994) Single unit (SUA) and group activity (MUA) in simulated populations of impulse coupled neurons with lateral inhibition. In: Elsner N, Breer H (eds) Sensory transduction. Göttingen Neurobiology Report 1994. Thieme, Stuttgart, p 864

Gray CM, König P, Engel AK, Singer W (1989) Oscillatory responses in cat visual cortex exhibit inter-columnar synchronization which reflects global stimulus properties. Nature 338:334–337

Hartmann G, Drüe S (1990) Self organization of a network linking features by synchronization. In: Eckmiller R, Hartmann G, Hauske G (eds) Parallel processing in neural systems and computers. Elsevier, Amsterdam, pp 361–364

Hebb DO (1949) The organization of behaviour. Wiley, New York

Hemmen JL van, Gerstner W, Ritz R (1992) A 'microscopic' model of collective oscillations in the cortex. In: Taylor JG, Caianiello ER, Cotterill RMJ, Clark JW (eds) Neural network dynamics. Springer, Berlin Heidelberg New York, pp 250-257

Kirillov AB, Woodward DJ (1993) Synchronization of spiking neurons: transmission delays, noise and NMDA receptors. In: Proceedings of the World Congress on Neural Networks, Portland, OR, pp 594–597

König P, Schillen TB (1991) Stimulus-dependent assembly formation of oscillatory responses. I. Synchronization. Neural Comput 3: 155–166

Kraut U, Nischwitz A, Waschulzik T (1993) Temporal resolution: a critical parameter in simulations of pulse-coupled neural networks. In: Okabe Y (ed) Proceedings of the International Joint Conference on Neural Networks '93, Nagoya, Japan, pp 1116–1119

Kuramoto Y (1991) Collective synchronization of pulse-coupled oscillators and excitable units. Physica D 50:15–30

Lytton WW, Sejnowski TJ (1991) Simulations of cortical pyramidal neurons synchronized by inhibitory interneurons. J Neurophysiol 66:1059–1079

MacGregor RJ, Palasek RL (1974) Computer simulation of rhythmic oscillations in neuron pools. Kybernetik 16:79–86

Milner PM (1974) A model for visual shape recognition. Psychol Rev 81:521–535

Mirollo RE, Strogatz SH (1990) Synchronization of pulse-coupled biological oscillators. SIAM J Appl Math 50:1645–1662

Niebur E, Schuster HG, Kammen DM (1991) Collective frequencies and metastability in networks of limit-cycle oscillators with time delay. Phys Rev Lett 67:2753–2756

Nischwitz A (1994) Impuls-Synchronisation in neuronalen Netzwerken. Harri Deutsch, Thun

Nischwitz A, Glünder H (1992) Gibt es ein zur starken Wechselwirkung analoges Prinzip bei der neuronalen Informationsverarbeitung? In: Krönig D, Lang M (eds) Physik und Informatik – Informatik und Physik. Springer, Berlin Heidelberg New York, pp 143–144

Nischwitz A, Glünder H (1993) Letter to the editor. Spektrum Wiss, no 1:8

Nischwitz A, Glünder H, Klausner P (1991) Synchronization of spikes in populations of laterally coupled model neurons. In: Kohonen T, Mäkisara K, Simula O, Kangas J (eds) Artificial neural networks 1. Elsevier, Amsterdam, pp 1771–1774

Nischwitz A, Glünder H, Oertzen A von, Klausner P (1992) Synchronization and label-switching in networks of laterally coupled model neurons. In: Aleksander I, Taylor J (eds) Artificial neural networks 2. Elsevier, Amsterdam, pp 851–854

Peskin CS (1975) Mathematical aspects of heart physiology. Courant Institute of Mathematical Sciences, New York University, New York

Pittendrigh CS, Bruce VG (1957) An oscillator model for biological clocks. In: Rudnick D (ed) Rhythmic and synthetic processes in growth. Princeton University Press, Princeton, NJ, pp 75–109

Pöppel E (1971) Oscillations as possible basis for time perception. Stud Gen 24:85–107

Rall W (1964) Theoretical significance of dendritic trees for neuronal input-output relations. In: Reiss RF (ed) Neural theory and modelling. Stanford University Press, Stanford, CA, pp 73–97

Sayer RJ, Friedlander MJ, Redman SJ (1990) The time course and amplitude of EPSPs evoked at synapses between pairs of CA3/CA1 neurons in the hippocampal slice. J Neurosci 10:826–836

Schuster HG, Wagner P (1989) Mutual entrainment of two limit cycle oscillators with time delayed coupling. Prog Theor Phys 81: 939–945

Sejnowski TJ, Lytton WW (1992) Inhibitory interneurons can synchronize cortical pyramidal neurons. In: Elsner N, Richter DW (eds) Rhythmogenesis in neurons and networks. Thieme, Stuttgart, pp 173–185

Smith LS, Cairns DE, Nischwitz A (1994) Synchronization of integrate-and-fire neurons with delayed inhibitory lateral connections. In: Marinaro M, Morasso PG (eds) Proceedings of the International Conference on Artificial Neural Networks '94. Springer, Berlin Heidelberg New York, pp 142–145

Traub RD, Miles R, Wong RKS, Schulman LS, Schneiderman JH (1987) Models of synchronized hippocampal bursts in the presence of inhibition. II. Ongoing spontaneous population events. J Neurophysiol 58:752–764

Vreeswijk C van, Abbott LF, Ermentrout GB (1994) When inhibition not excitation synchronizes neural firing. J Comput Neurosci 1:313–321

Wang X, Blum EK (1992) Discrete-time versus continuous-time models of neural networks. J Comput Syst Sci 45:1–19

Wiener N (1961) Cybernetics or control and communication in the animal and the machine. MIT Press, Cambridge, MA